Research Article

Raghad U. Abass*, Mohammed Ausama Al-Sarraf, Dandi Bachtiar and Mohd Ruzaimi Bin Mat Rejab

Eco-friendly mechanical performance of date palm Khestawi-type fiber-reinforced polypropylene composites

https://doi.org/10.1515/jmbm-2024-0019
received September 04, 2024; accepted October 02, 2024

Abstract: Natural sources used in industry, such as environmental waste fibers for plants, waste paper, and others, can lessen waste-throwing problems and reduce environmental pollution to save lives on the earth's crust. The natural composites of natural fiber-reinforced thermoplastic are undoubtedly to be sustainable and eco-friendly. Therefore, the current work was conducted to study the addition of natural fiber date palm Khestawi-type fiber (DPKF) with different loadings (5, 10, and 15%) into the polypropylene (PP) matrix to prepare DPKF/PP composites. The specimens were prepared by using the lamination method. In addition, the mechanical properties of these composite material specimens were studied by following ASTM, which included tensile, flexural, and impact tests. A scanning electron microscope (SEM) and X-ray diffraction (XRD) were employed to analyze the morphology and the structure crystallite studied of the DPKF/PP composites. The results show that the DPKF/PP composite with 15% fiber content recorded the best tensile strength, tensile modulus, and low tensile strain performance. Moreover, XRD and SEM analysis confirmed the mechanical properties and crystalline nature of the DPKF/PP composites. Finally, the values of the flexural and impact properties increased with increasing fiber loading.

Keywords: date palm Khestawi-type fiber, polypropylene matrix, mechanical properties, lamination, materials characterizations

*** Corresponding author: Raghad U. Abass**, Applied Sciences Department, University of Technology-Iraq, Baghdad, Iraq, e-mail: Raghad.U.Abass@uotechnology.edu.iq
Mohammed Ausama Al-Sarraf: Department of Materials Engineering, University of Technology-Iraq, Baghdad, Iraq
Dandi Bachtiar: Department of Mechanical and Industrial Engineering, Universitas Syiah Kuala, Kopelma Darussalam, Banda Aceh, Indonesia
Mohd Ruzaimi Bin Mat Rejab: Faculty of Mechanical Engineering, Universiti Malaysia Pahang Al-Sultan Abdullah (UMPSA), 26600, Pekan, Pahang, Malaysia

1 Introduction

Each engineering application or engineering design has a set of crucial factors that need to be achieved to get proper design successfully [1–5]. Global and governmental trends have commanded that subrogated industrial materials by sustainable and environmentally friendly materials [6–9]. Therefore, the process of selecting sustainable materials and the method of manufacturing are considered crucial factors in achieving the sustainable development goals of the "British Times Organization" [10–15]. For engineering applications, the right balance between the material's performance, recyclability, and functionality became crucial. Furthermore, discovering new materials with appealing, unique properties might open up new avenues for design [16–19]. However, lots of requirements and restrictions often affect the use of a particular type of material in a specific application [20–22]. As a result, choosing the right material type for a given application is a multi-criteria problem where appropriate judgments must be made for each design based on several special factors [23].

The use of natural resources has been strongly encouraged recently due to the enormous need for awareness of environmental impact [24]. This has pushed the government's emphasis on new regulations regarding environmental impact issues and sustainability concepts, as well as growing social, economic, and ecological awareness [25–27]. As a result, natural fiber composites, also known as natural fiber reinforced polymer composites or NFRPCs, emerged as a useful substitute material type for a variety of applications [28]. Traditionally, constructed fibers have been employed as reinforcing components in composite materials [29]. Meanwhile, there is currently interest in replacing them with natural fibers [30–35]. As fillers or reinforcing elements for polymer-based matrices, natural fiber composites, including jute [36], date palm fiber [37], hemp [38], sisal [39], oil palm fiber [40], kenaf [41], sugar palm fiber [42], and flax [43] are used. Using natural fibers in this method reduces waste disposal issues and environmental degradation, and the sustainable goal can be achieved [44].

NFCs have several advantages over synthetic composites, like low costs and density and acceptable specific strength and modulus, which can lead to low-weight products [45,46]. Since they are generated from a renewable resource, their production requires less energy, and unlike glass fibers, they may be simply disposed of at the end of their useful life by composting or by recovering their calorific value in a furnace [47]. Furthermore, natural fibers are superior to conventional glass fibers in several ways, including availability, sequestration of CO_2, improved energy recovery, less tool wear during machining, and decreased irritation of the skin and respiratory system [48–51].

Except for the northern region, Iraq may be regarded as a date palm country because date palm trees are found throughout the place. Iraq has a wide variety of date palm tree species [48]. Zahidi, Khastawi, Barhi, Berban, Khadrawi, *etc.*, are among them. Date palms of the Khestawi kind are conveyed to be the best because their fruits have a sweet flavor taste [52]. Owing to the abundance of these trees, a significant amount of fiber could be obtained [53–55].

There are several processes used for manufacturing composite materials based on thermoplastics, such as extrusion, injection molding, internal mixing, heat pressing, lamination, *etc.* [56]. Choosing one of these methods is considered a great challenge, given that each of these methods has advantages and disadvantages [57]. Extrusion in the manufacture of plastics is beset by issues with quality control, limited materials, and expensive setup expenses at first [58]. Enhancing process effectiveness and efficiency requires reducing waste and achieving consistent product quality [59–61]. Moreover, innovative solutions are needed to enhance process efficiency and product quality since internal mixers have drawbacks such as high-energy consumption, equipment wear, and difficulties establishing uniform mixing. These issues also impede scaling and raise operational expenses [62–65].

Conversely, the lamination process offers substantial advantages in terms of barrier qualities, customization, strength, aesthetic appeal, adaptability, material efficiency, and better functionality, whereas internal mixers and extruders encounter unique obstacles in the manufacturing of plastics. Thus, the lamination process has a positive effect on the mechanical properties of date palm Khestawi type fiber (DPKF)/polypropylene (PP) composites as it reduces the effect of heat and thereby holds the internal structure of the fibers and the polymer together, improving the mechanical performance compared to other manufacturing techniques such as extrusion the composite is subjected to repeated heat.

Therefore, in this study, a lamination technique was utilized to prepare all dosages of DPKF/PP composites. After that, their performance was evaluated by testing their tensile, flexural, and impact properties, which were then characterized by X-ray diffraction (XRD) and scanning electron microscopy (SEM). This composite material can be applied in several industries, such as automotive, packaging, and others.

2 Experimental procedure

2.1 Materials

The materials used in this study were PP and DPKF. The matrix PP was purchased from Malaysia SDN BHD/Petronas Co. Ltd, with properties shown in Table 1. Date palm Khestawi-type fiber was obtained locally.

2.2 Preparation of fiber

The fiber was washed in tap water to remove impurities and dust and then dried for 2 days at atmosphere pressure and room temperature. Afterwards, the fiber was put in the oven at 80°C for 24 h to complete the drying process and remove the moisture.

2.3 Preparation of DPKF/PP composites

The lamination method was carried out by producing sheets of thermoplastic PP with dimensions of 20 cm × 20 cm and a thickness of 1 mm for subsequent preparation for various DPKF/PP composites using a hot press machine model ILLIG RD 53C, 10 tons (Figure 1). The first stage was produced sheets with a thickness of 1 mm. Two molds with the same dimensions were used of different thicknesses.

Table 1: PP properties [26]

Product properties	Test method	Units	Value
Melt flow rate (230°C/2.16 kg)	ISO 1133	g/10 min	12
Flexural modulus	ISO 178	MPa	1,300
Tensile stress at yield	ISO 527	MPa	32
Specific gravity	ISO 1183	g/cm^3	0.855
Melting temperature	ISO 11357-3	°C	160
Izod notched at 23°C min*	ISO 180/1A	kJ/m^2	2.5

*Injection molding procedure for a specimen as per ISO 180/1A.

The molds were made of stainless steel with dimensions of 20 cm × 20 cm, 1-mm-thick (the initial mold for producing the sheets), and the other 3 mm thick (the final mold for composites) with a top and bottom cover. The number of layers was fixed at three for all the DPKF/PP composites studied, and fibers were added between them. The heating process with a hot press was carried out by placing the mold inside the hot press machine after the required amount of polymer or polymer sheets and fibers. To produce the composites DPKF/PP, a layer of sheets was added to the bottom of the mold, half the amount of DPKF reinforcement was added, and another layer of sheets was added, after which the final amount of fibers, subsequently the last layer. The mold was closed with the upper cover and then inserted into the hot pressing machine to apply a mechanical load of 4 tons and a constant thermal load for all operations of 165°C. The mold was placed in a hot press machine for 12 min before the heating stopped. Then cooling began at 10°C/min until around 30°C, before the mold was released. In the final stage of the process, the composite sheets were cut using a manual cutting saw according to the standard specifications for tension, bending, and impact.

3 Mechanical tests of DPKF/PP composites

3.1 Tensile test

Tensile tests determine a material's behavior to stress by applying tensile (pulling) force on it. Testing a material's strength and elongation ability is how tensile tests do this. This test was performed according to (ASTM D638). The test gives the full material profile tensile properties (strength, modulus, strain). The relation between stress and strain, which was obtained gives the composites' mechanical behavior during the load and predicts the point of failure. Instron Laryee (Figure 2) was used with a crosshead speed of 5 mm/min. Five specimens were prepared for each composite.

3.2 Flexural test

Bend testing establishes a material's flexural strength and modulus by applying stress to it until it fractures or deforms. Shear stress is created along the midline of the specimen during a flexure test, which causes tensile tension on the convex side and compression stress on the concave side. Shear stress needs to be reduced to guarantee that tensile or compression stress is the main cause of failure [3]. The same INSTRON in tensile test performed this test according to ASTM D790.

3.3 Impact test

Impact testing is the process of evaluating the resistance of an item to high-speed loading. An impact test measures the amount of energy required to fracture a test item quickly. This test is performed according to ISO-180 [3]. When the

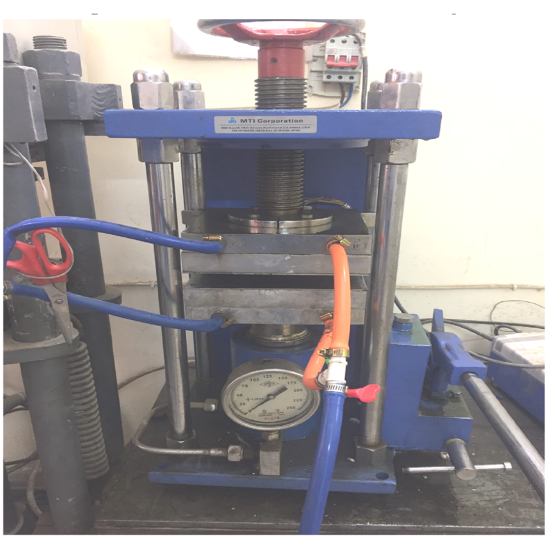

Figure 1: Hot press machine model ILLIG RD 53C, 10 tons.

Figure 2: Tensile Instron Laryee.

Figure 3: Pendulum XJU-22 Izod impact test.

specimen is clamped at one end and held vertically in a cantilever beam end, it breaks at a velocity of 3.5 m/s due to a pendulum XJU-22 (Figure 3) with a work value of 5.5 J.

In addition, all the mechanical specimens were tested five times for each tensile, flexural, and impact properties test individually. Accordingly, Table 2 represents the tensile properties, and Table 3 illustrates the impact and flexural properties of the DPKF/PP composites. Moreover, the crucial statistical factors were calculated accordingly to represent the average, error, and standard deviation for each DPKF/PP composite sample.

4 Characterizations of DPKF/PP composites

4.1 SEM

A sophisticated kind of electron microscope called a SEM uses a focused electron beam to scan a sample's surface to produce precise photographs of its surface. High-resolution pictures that show the topography and surface composition of the sample are made possible in large part by the SEM. SEM is utilized in the context of composite materials to see how various contents, such as DPKF (a particular filler or addition), affect the fracture surface following a tensile test for the DPKF/PP composites. The SEM Tescan Mira3 XMU from the Czech Republic (Figure 4) was the particular equipment utilized for this observation. Understanding how different DPKF concentrations affect the mechanical characteristics and failure causes of the composites was made easier with this technique.

4.2 XRD

By examining their distinct diffraction patterns, crystalline materials may be quickly and accurately characterized through the use of XRD, an analytical method that aids in the identification of various phases within the material. One such piece of equipment is the Shimadzu, Japan-based XRD-6000 device. A crystalline sample, such as a DPKF sample, reacts to X-rays by producing constructive interference patterns. The structural details of the sample are then revealed by detecting, processing, and recording these diffracted X-rays (Figure 5).

5 Results and discussion

5.1 Effect of changed fiber content on the tensile properties of DPKF/PP composites

5.1.1 Tensile strength

Figure 6 shows the effect of fiber loading on the tensile strength of DPKF/PP composites. The tensile strength values for the neat PP, 5, 10, and 15 wt% of DPKF/PP composites were 30.54, 27.844, 25.87, and 32.2 MPa, respectively. The best composite was the third one with a content of 15 wt% DPKF in the PP matrix. This was due to the good distribution of fibers within the matrix [27,66–70], and the perfect match between the fibers added with the polymer [28,71–75], reflected in its cohesion as obvious in Figure 8d. In addition, there were no gaps or voids between the fibers and the polymer, producing heavy interlocking [9,76–78]. Therefore, this proves that mechanical interlocking was sufficient to transfer the load from PP to DPKF, and the reinforcing effect of the DPKF was dominant. Meanwhile, at 5, 10 wt%, DPKF/PP composites, the less fiber amount in the matrix caused a reduction in load transfer capacity among the fibers; the lack of fiber content pushed the accumulation of stresses and reduced their transfer in the structure of the composites, which weakened their ability to withstand, so they failed [28,79–83].

5.1.2 Tensile modulus

Figure 7 shows the effect of fiber content on the tensile modulus of DPKF/PP composites. The tensile modulus values for the neat PP, 5, 10, and 15 wt% of DPKF/PP composites were 4.81, 5.708, 5.25, and 8.49 GPa, respectively. The tensile modulus of DPKG/PP composites augmented gradually with the fiber loading doses. The composite consists of a low-stiffness matrix and high-stiffness fibers; therefore, the increasing fiber loading leads to a rise in the stiffness of composites [29].

Table 2: Tensile strength, tensile modulus, tensile strain, average, error, and standard deviation for the neat PP and different DPKF content by weight percentage in DPKF/PP composites

No. of samples	Different DPKF content wt% in PP	Tensile strength (MPa)	Tensile modulus (GPa)	Tensile strain (%)
1	(1) 0% DPKF with neat PP	30.132	5.27	7.322
2	(2) 0% DPKF with neat PP	36.247	4.66	6.459
3	(3) 0% DPKF with neat PP	34.311	5.70	5.706
4	(4) 0% DPKF with neat PP	26.308	4.09	6.5
5	5) 0% DPKF with neat PP	25.702	4.34	5.913
	Average	30.54	4.81	6.38
	Std.error	2.1009	0.2343	0.2811
	Std.Dev.E	4.6977	0.5240	0.6286
	Error	−2.5968	−0.2897	−0.347
1	(1) 5% DPKF with 95% PP	24.081	6.371	5.386
2	(2) 5% DPKF with 95% PP	27.584	5.355	4.211
3	(3) 5% DPKF with 95% PP	26.162	5.778	5.292
4	(4) 5% DPKF with 95% PP	32.838	5.067	5.578
5	(5) 5% DPKF with 95% PP	28.555	5.969	3.896
	Average	27.844	5.708	4.87
	Std.error	1.4578	0.2289	0.3412
	Std.Dev.E	3.2597	0.5119	0.7630
	Error	−1.8019	−0.2830	−0.4218
1	(1) 10% DPKF with 90% PP	28.51	4.834	4.597
2	(2) 10% DPKF with 90% PP	26.258	5.079	5.621
3	(3) 10% DPKF with 90% PP	26.885	4.636	4.668
4	(4) 10% DPKF with 90% PP	21.423	5.693	4.795
5	(5) 10% DPKF with 90% PP	26.274	6.008	4.769
	Average	25.87	5.25	4.89
	Std.error	1.1851	0.2598	0.1862
	Std.Dev.E	2.6500	0.5810	0.4163
	Error	−1.4649	−0.3212	−0.2301
1	(1) 15% DPKF with 85% PP	34.332	7.589	4.163
2	(2) 15% DPKF with 85% PP	31.359	8.738	3.751
3	(3) 15% DPKF with 85% PP	27.35	9.326	4.113
4	(4) 15% DPKF with 85% PP	37.154	8.592	3.182
5	(5) 15% DPKF with 85% PP	30.805	8.205	3.741
	Average	32.2	8.49	3.79
	Std.error	1.6623	0.2884	0.1756
	Std.Dev.E	3.7170	0.6449	0.3928
	Error	−2.0547	−0.3565	−0.2171

where Std.error: standard error, Std.Dev.E: standard deviation.

5.1.3 Tensile strain

Figure 8 shows the effect of fiber range on the tensile strain of DPKF/PP composites. The tensile strain values for the pure PP, 5, 10, and 15 wt% of DPKF/PP composites were recorded as 6.38, 4.87, 4.89, and 3.79%. DPKG/PP composites' tensile strain declined slowly due to increased fiber loading. This supported the tensile modulus property of the DPKF/PP composites. Due to increased fiber content instead of increased polymers, composites tend to be less stretchable when compared with the neat PP matrix. This is due to the superior elongation ability of PP compared to the low capability of elongation for reinforced fibers in composites [30]. As a result of orientation, the fibers in the matrix parallel to the line of tensile stress resulted in high stiffness with a noticeable decrease in elongation [31].

5.2 Effect of changed fiber content on the flexural properties of DPKF/PP composites

5.2.1 Flexural strength

Figure 9 shows the effect of fiber lamination content on the flexural strength of DPKF/PP composites. The flexural

Table 3: Flexural strength, flexural modulus, impact strength, average, error, and standard deviation for the neat PP and different DPKF content by weight percentage in DPKF/PP composites

No. of samples	Different DPKF content wt% in PP	Flexural modulus (GPa)	Flexural strength (MPa)	Impact strength (%)
1	(1) 0% DPKF with neat PP	0.233	19.74	20.9
2	(2) 0% DPKF with neat PP	0.189	21.08	22.131
3	(3) 0% DPKF with neat PP	0.172	21.84	28.258
4	(4) 0% DPKF with neat PP	0.205	21.10	29.026
5	(5) 0% DPKF with neat PP	0.201	16.26	27.685
	Average	0.2	20	25.6
	Std.error	0.0100	0.4755	1.6922
	Std.Dev.E	0.0225	1.0632	3.7840
	Error	−0.0124	−0.5877	−2.0917
1	(1) 5% DPKF with 95% PP	0.65	35.202	9.939
2	(2) 5% DPKF with 95% PP	0.474	30.963	10.148
3	(3) 5% DPKF with 95% PP	0.617	41.896	10.86
4	(4) 5% DPKF with 95% PP	0.515	38.973	9.365
5	(5) 5% DPKF with 95% PP	0.689	38.681	10.688
	Average	0.589	37.143	10.2
	Std.error	0.0407	1.8744	0.2685
	Std.Dev.E	0.0911	4.1912	0.6004
	Error	−0.0504	−2.3168	−0.3319
1	(1) 10% DPKF with 90% PP	0.682	43.395	17.745
2	(2) 10% DPKF with 90% PP	0.621	35.901	16.244
3	(3) 10% DPKF with 90% PP	0.552	41.667	13.608
4	(4) 10% DPKF with 90% PP	0.66	32.476	17.044
5	(5) 10% DPKF with 90% PP	0.62	46.561	18.359
	Average	0.627	40	16.6
	Std.error	0.0222	2.5570	0.8271
	Std.Dev.E	0.0496	5.7176	1.8494
	Error	−0.0274	−3.1606	−1.0223
1	(1) 15% DPKF with 85% PP	1.122	63.034	24.54
2	(2) 15% DPKF with 85% PP	1.286	66.883	17.59
3	(3) 15% DPKF with 85% PP	1.305	55.141	19.555
4	(4) 15% DPKF with 85% PP	0.975	59.242	20.84
5	(5) 15% DPKF with 85% PP	0.957	55.7	25.975
	Average	1.129	60	21.7
	Std.error	0.0738	2.2277	1.5584
	Std.Dev.E	0.1651	4.9813	3.4848
	Error	−0.0912	−2.7536	−1.9263

where Std.error: standard error, Std.Dev.E: standard deviation.

strength values for the neat PP, 5, 10, and 15 wt% of DPKF/PP composites were 20, 37.143, 40, and 60 MPa, respectively. Flexural strength showed an increasing trend as fiber lamination loadings increased. The strong bonding between DPKF and PP matrix resulted in thriving flexural behaviors where the performance of the stress conveyed between the polymer and fiber rose. A similar behavior was also observed by teams of investigators [32–35].

5.2.2 Flexural modulus

Figure 10 shows the effect of fiber content on the flexural modulus of DPKF/PP composites. The flexural modulus values for the neat PP, 5, 10, and 15 wt% of DPKF/PP composites were 0.2, 0.589, 0.627, and 1.129 GPa, respectively. There was a similar behavior between flexural modulus and flexural strength. This confirmed the flexural strength results, as proved previously by [32–35].

5.3 Effect of changed fiber content on the impact strength of DPKF/PP composites

Figure 11 shows the effect of fiber content on the average impact strength of DPKF/PP composites. The impact

Figure 4: SEM Tescan Mira3 XMU from the Czech Republic.

Figure 5: Shimadzu, Japan-based XRD-6000 device.

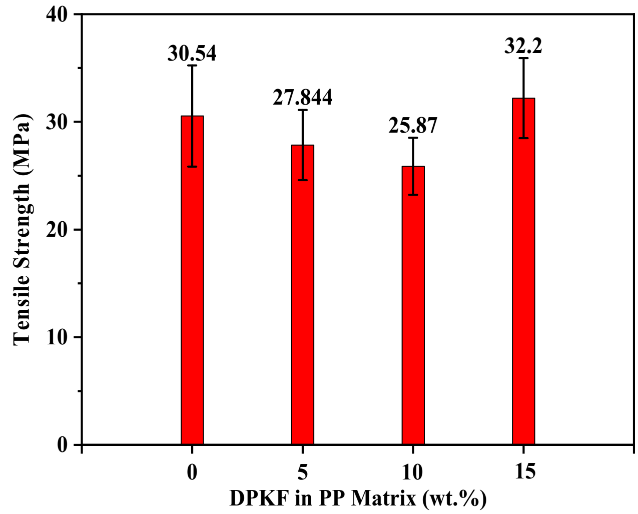

Figure 6: Effect of fiber loading on tensile strength of DPKF/PP composites.

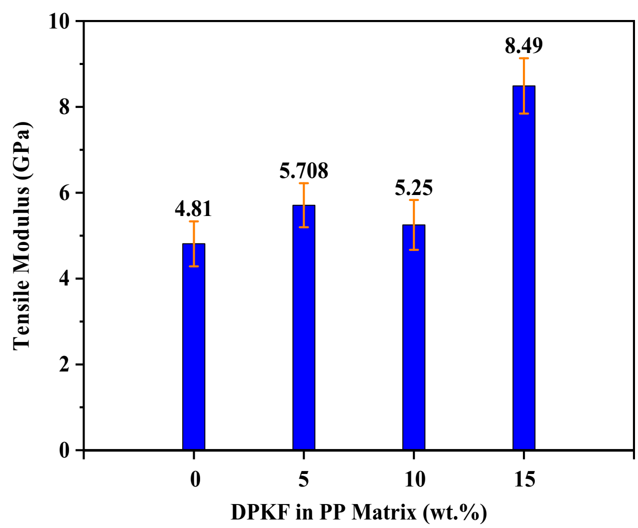

Figure 7: Effect of fiber loading on tensile modulus of DPKF/PP composites.

strength values for the neat PP, 5, 10, and 15 wt% of DPKF/PP composites were 25.6, 10.2, 16.6, and 21.7 kJ/m^2, respectively. It was evident that, when compared with the other composites at various energy levels, the composite specimens with 15% DPKF loading had greater impact strength values. It could be attributed to the increase in the stiffness of the composite due to the increased DPKF loading of reinforced PP. Conversely, there was a deterioration in impact strength behaviors for all doses of DPKF/PP when compared with the highest impact strength recorded for PP. When the hummer strikes the test sample, it undergoes kinetic energy dissipation through several processes, according to the energy dissipation point of view. For instance, these mechanisms include pull-out, tension, deformation, and frictional slip of DPKF in the PP matrix. Many factors dominate the impact process, such as hummer shape, fiber properties, and boundary conditions, the most critical of which is temperature. Therefore, the reason for the decline in impact strength values for all doses of DPKF/PP may be due to the influence of the temperature at which the test was performed [36].

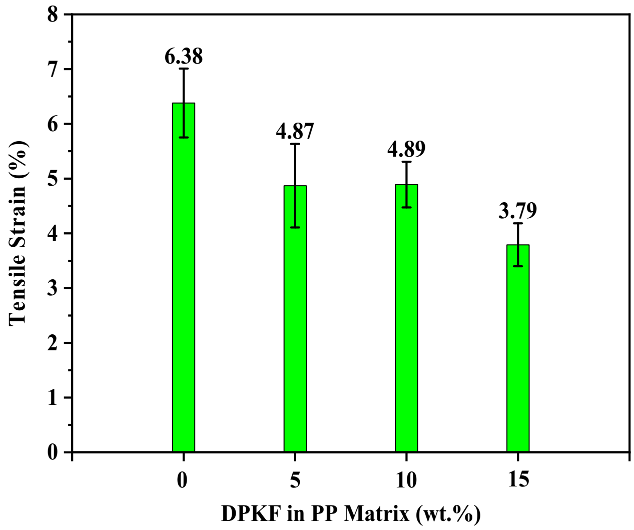

Figure 8: Effect of fiber loading on the tensile strain of DPKF/PP composites.

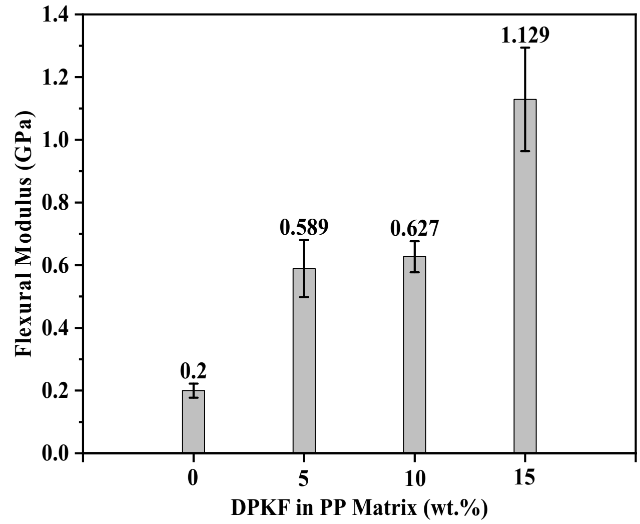

Figure 10: Effect of fiber loading on the flexural modulus of DPKF/PP composites.

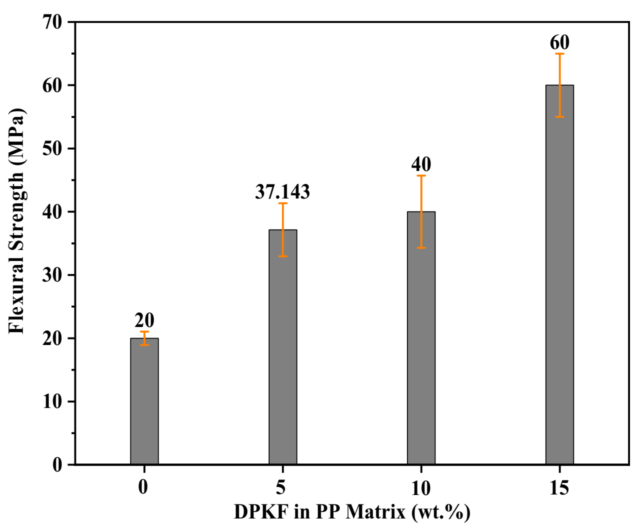

Figure 9: Effect of fiber loading on the flexural strength of DPKF/PP composites.

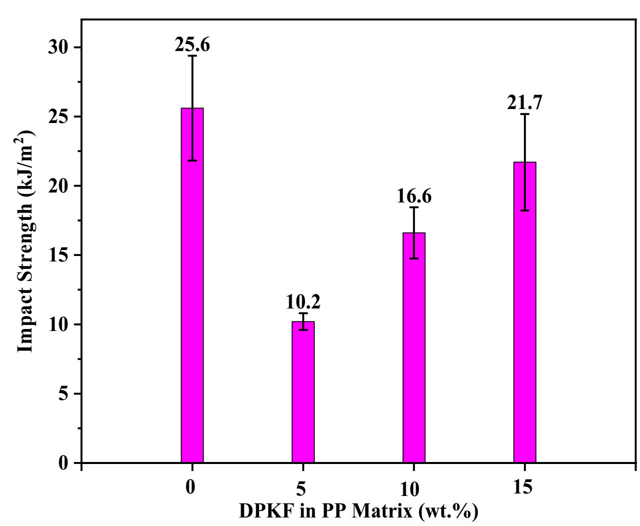

Figure 11: Effect of fiber loading on the impact strength of DPKF/PP composites.

6 Characterizations of DPKF/PP composites with changing fiber content

6.1 SEM

Figure 12 shows the SEM images for the fracture surfaces of tensile specimens for the different fiber content of DPKF in DPKF/PP composites. The pull-out and breakage of all DPKF combinations in the PP matrix were detected. This indicated that the adhesion between DPKF and PP matrix was good.

Figure 12a shows a streamlined, glassy broken surface in different places of the structured PP matrix.

Figure 12b–d show moderate fiber-matrix adhesion, with some gaps between fibers and matrix due to the hydrophilicity nature of DPKF, which was affected by heating processes during the hot compression procedures. In addition, SEM detected crushing and pulling-out fibers in different areas of the DPKF/PP composites due to the good interlocked DPKF with PP polymers [37–39]. Finally, this analysis confirmed the mechanical behaviors of the different DPKF/PP composites, such as tensile, flexural, and impact properties, as shown in Figure 6, through the precise representation of the fracture area in Figure 12.

6.2 XRD

Figure 13 shows the XRD analysis for the pure PP and changed fiber loading 5, 10, and 15 wt% of DPKF/PP composites. For the pure PP and the group DPKF/PP composites, the highest peak was found at $2\theta = 14.1°$; meanwhile, the lowest was at $2\theta = 18.64°$. Conversely, the intensities for these dosages were recorded as PP = 842.61, with different DPKF loading 5, 10, and 15 wt% in the PP matrix as 776.94, 777.14, and 880.05, respectively. The high-intensity peaks commonly indicate a coherent crystalline structure. However, the low intensity confirms disorderly interaction in the crystal structure. In other words, the intensity reflects the crystallinity of composites [40]. Relying on that consideration the 15 wt% DPKF/PP composite proved the best mechanical properties among all the DPKF/PP dosages and PP matrix. Additionally, DPKF distribution was uniformly noted in the form of individual layers within the PP polymer, causing exfoliated DPKF/PP composites with upgraded properties [1].

XRD data for pure PP and its composites reinforced with different percentages of DPKF is shown in the following tables. For material crystalline structure and phase behavior analysis, 2θ, d-spacing, and full width at half maximum (FWHM) measurements are essential.

Table 4 describes pure PP's XRD features, whereas Tables 5–7 show the impacts of adding 5, 10, and 15 wt% DPKF to the PP matrix. These comparisons show how

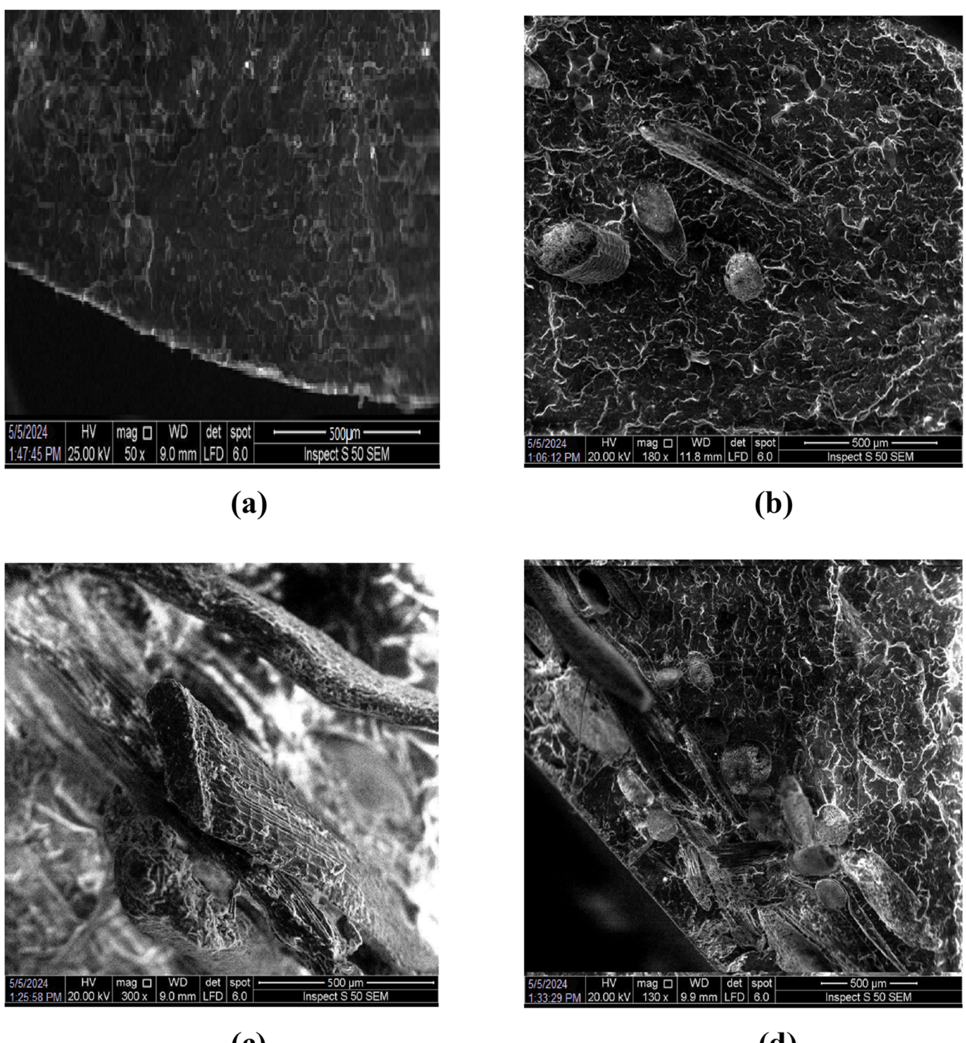

Figure 12: SEM images of (a) pure PP, (b) 5 wt%, (c) 10 wt%, and (d) 15 wt% DPKF/PP composites.

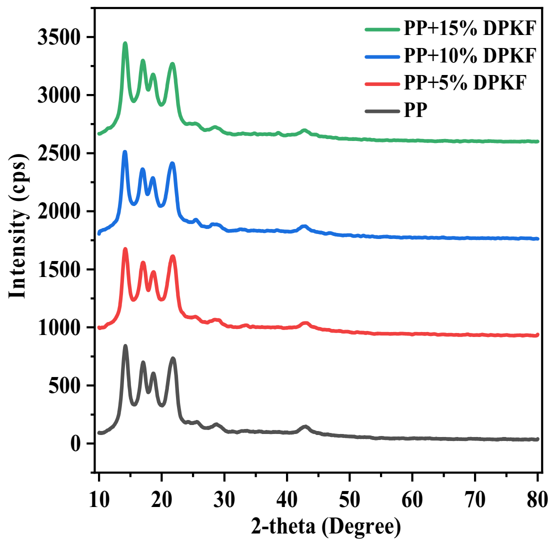

Figure 13: Diffraction pattern of pure PP and different DPKF/PP composites.

Table 4: XRD data showing 2*θ*, *d*-spacing, and FWHM for pure PP

2*θ* (deg)	*d* (Å)	FWHM (deg)	Intensity (counts)	Crystallite size (nm)
14.2757	6.19925	1.16040	17,264	6.91
21.6862	4.09472	1.65600	18,564	4.89
17.0978	5.18185	1.36800	13,720	5.88
14.2757	6.19925	1.16040	17,264	6.91
17.0978	5.18185	1.36800	13,720	5.88
18.7468	4.72960	1.31560	11,179	6.13
21.6862	4.09472	1.65600	18,564	4.89
25.6898	3.46494	0.96000	1,308	8.49
28.8781	3.08923	1.42670	1,233	5.75
42.8386	2.10931	1.66670	2,235	5.12
Average				6.08

Table 5: XRD data showing 2*θ*, *d*-spacing, and FWHM for 5 wt% DPKF reinforced PP composites

2*θ* (deg)	*d* (Å)	FWHM (deg)	Intensity (counts)	Crystallite size (nm)
14.2932	6.19170	1.20780	14,156	6.63
21.6581	4.09997	1.72960	17,586	4.68
17.0699	5.19026	1.56000	13,556	5.15
11.6883	7.56510	0.82660	242	9.67
12.5639	7.03977	1.12000	1,373	7.14
14.2932	6.19170	1.20780	14,156	6.63
17.0699	5.19026	1.56000	13,556	5.15
18.6671	4.74961	1.68000	11,780	4.80
21.6581	4.09997	1.72960	17,586	4.68
25.1707	3.53521	1.96000	2,464	4.16
28.6185	3.11666	1.86670	1,563	4.40
33.3795	2.68220	0.84000	477	9.88
42.9319	2.10494	1.76000	1,805	4.85
44.3111	2.04257	0.88000	463	9.75
Average				6.26

Table 6: XRD data showing 2*θ*, *d*-spacing, and FWHM for 10% DPKF-reinforced PP composites

2*θ* (deg)	*d* (Å)	FWHM (deg)	Intensity (counts)	Crystallite size (nm)
14.1909	6.23610	1.11090	15,258	7.21
21.5895	4.11284	1.62200	16,369	4.99
17.0300	5.20233	1.50000	12,554	5.36
11.4497	7.72220	1.20000	582	6.66
14.1909	6.23610	1.11090	15,258	7.21
17.0300	5.20233	1.50000	12,554	5.36
18.5872	4.76985	1.52000	10,501	5.30
21.5895	4.11284	1.62200	16,369	4.99
25.3370	3.51238	1.29330	1,646	6.30
28.6751	3.11064	1.78000	1,346	4.61
42.7087	2.11543	1.55330	1,909	5.50
Average				5.77

reinforcing affects composites' crystalline structure and mechanical characteristics.

7 Conclusion

An environmentally friendly composite of the DPKF/PP with a meticulously selected lamination method for its generation successfully achieved good mechanical properties.

The mechanical tensile, flexural, and impact properties studies confirmed the best fiber loading content of 15 wt% DPKF/PP that recorded a peak of tensile strength at a value of 32.2 MPa. Moreover, the recording was supported and confirmed by the SEM and XRD analyses as well. The highest peak for both the pure PP and the group DPKF/PP composites was found at 2θ = 14.1°, while the lowest peak was found at 2θ = 18.64°. However, the intensities with varying DPKF

Table 7: XRD data showing 2*θ*, *d*-spacing, and FWHM for 15% DPKF reinforced PP composites

2*θ* (deg)	*d* (Å)	FWHM (deg)	Intensity (counts)	Crystallite size (nm)
14.2814	6.19679	1.20090	16,116	6.97
17.0699	5.19026	1.68000	15,740	5.00
21.5939	4.11202	1.80890	18,729	4.67
11.6883	7.56510	1.09340	692	7.63
12.6834	6.97371	1.04000	2,048	8.03
14.2814	6.19679	1.20090	16,116	6.97
17.0699	5.19026	1.68000	15,740	5.00
18.6671	4.74961	1.68000	12,242	5.01
21.5939	4.11202	1.80890	18,729	4.67
25.2905	3.51873	1.76000	1,507	4.83
28.6851	3.10958	1.52000	1,178	5.64
42.7521	2.11338	1.52000	1,740	5.86
44.5510	2.03213	0.88000	542	10.19
Average				6.19

loadings of 5, 10, and 15 wt were noted for these dosages, with PP = 842.61% as 776.94, 777.14, and 880.05, in the PP matrix, in that order. This composite can be used in the automotive industry due to it is considered a sustainable material. We recommend further research to explore other applications of this material in different fields of engineering. This composite may need study with different combination methods or may need fiber treatment to improve the mechanical properties. These if applied could open many fields to utilize these composites in other application domains.

Acknowledgments: The Ministry of Higher Education and Scientific Research (MHESR) of the Iraqi Republic and the University of Technology-Iraq (UOT) provided assistance for this work. Moreover, the author is thankful to the Applied Science Department, Universitas Syiah Kuala in Indonesia and Universiti Malaysia Pahang in Malaysia for all its support.

Funding information: This research did not receive any specific funding from any university or external funding agencies in the public, commercial, or not-for-profit sectors. It was conducted independently as part of the authors' academic work.

Author contributions: In this study, Raghad U. Abass conceptualized and designed the research, prepared the DPKF/PP composite specimens using the lamination method, and conducted mechanical testing, including tensile, flexural, and impact tests, following ASTM standards. Mohammed Ausama Al-Sarraf supported the specimen preparation and mechanical testing processes while also performing SEM and XRD analyses to assess the morphology and crystallinity of the composites. Dandi Bachtiar contributed to the experimental methodology and data analysis, providing insights into the mechanical behavior of the composites and validating the findings related to fiber-matrix interactions. Mohd Ruzaimi Bin Mat Rejab was responsible for statistical analysis and visualization of the data, including creating figures and tables, and assisted in the final editing and reviewing of the manuscript for submission. All authors have accepted responsibility for the entire content of this manuscript and consented to its submission to the journal, reviewed all the results and approved the final version of the manuscript.

Conflict of interest: The authors state no conflict of interest.

Data availability statement: The datasets generated during and/or analysed during the current study are available from the corresponding author on reasonable request.

References

[1] Mohammed AA, Bachtiar D, Siregar JP, Rejab MR, Hasany SF. Physicochemical study of eco-friendly sugar palm fiber thermoplastic polyurethane composites. BioResources. 2016;11(4):9438–54. doi: 10.15376/biores.11.4.9438-9454.
[2] Russell-Bennett R, Rosenbaum MS, Fisk RP, Raciti MM. SDG editorial: improving life on planet earth–a call to action for service research to achieve the sustainable development goals (SDGs). J Serv Mark. 2024 Jan;38(2):145–52.
[3] Azwa ZN, Yousif BF, Manalo AC, Karunasena W. A review on the degradability of polymeric composites based on natural fibres. Mater Des. 2013 May;47:424–42.
[4] Faruk O, Bledzki AK, Fink H-P, Sain M. Biocomposites reinforced with natural fibers: 2000–2010. Prog Polym Sci. 2012;37:1552–96.
[5] Kalia S, Kaith B, Kaur I. Cellulose fibers: bio-and nano-polymer composites: green chemistry and technology. Dordrecht, Heidelberg, London, New York: Springer Science & Business Media; 2011.
[6] Govindan K, Kaliyan M, Kannan D, Haq AN. Barriers analysis for green supply chain management implementation in Indian industries using analytic hierarchy process. Int J Prod Econ. 2014;147:555–68.
[7] Kandachar P. Opportunities for product development for industrial applications in polymers reinforced with natural fibres. In Proceedings of the Risø International Symposium on Materials Science. 2002. p. 15–33.
[8] Mohammed A, Bachtiar D, Rejab MR, Hasany S, Siregar J. Influence of different sugar palm fiber content on the tensile, flexural, impact, and physicochemical properties of eco-friendly thermoplastic polyurethane. Theor Found Chem Eng. 2019;53(3):454–62. doi: 10.1134/s0040579519030072.
[9] Singh H, Singh JIP, Singh S, Dhawan V, Tiwari SK. A brief review of jute fibre and its composites. Mater Today: Proc. 2018;5:28427–37.
[10] Haboubi C, Barhdadi EH, Haboubi K, Hammoudani YE, Sadoune Z, El Abdouni A, et al. Characterization of the mechanical behavior of hemp-clay composites. Adv Sci Technol Res J. 2024;18(2):71–7.
[11] Makinde-Isola BA, Taiwo AS, Oladele IO, Akinwekomi AD, Adelani SO, Onuh LN. Development of sustainable and biodegradable materials: a review on banana and sisal fibre based polymer composites. J Thermoplast Compos Mater. 2024;37:1519–39.
[12] Koeipudsa N, Phinyocheep P. Cellulose nanocrystals from oil palm trunk biomass as a bio-reinforcing filler for improved mechanical properties of modified natural rubber composites. Polym Compos. 2024;45(5):4524–37.
[13] Asyraf MRM, Sheng DD, Mas' ood NN, Khoo PS. Thermoplastic composites reinforced chemically modified kenaf fibre: current progress on mechanical and dynamic mechanical properties. Biomass Convers Biorefin. 2024;1–21.
[14] Alipour A, Jayaraman K. Performance of flax/epoxy composites made from fabrics of different structures. Fibers. 2024;12:34.
[15] Alves C, Silva A, Reis L, Freitas M, Rodrigues L, Alves D. Ecodesign of automotive components making use of natural jute fiber composites. J Clean Prod. 2010;18:313–27.
[16] Al-Oqla FM, Sapuan S. Natural fiber reinforced polymer composites in industrial applications: feasibility of date palm fibers for sustainable automotive industry. J Clean Prod. 2014;66:347–54.
[17] Sarikanat M. The influence of oligomeric siloxane concentration on the mechanical behaviors of alkalized jute/modified epoxy composites. J Reinf Plast Compos. 2010;29:807–17.

[18] Adamu M, Alanazi H, Ibrahim YE, Abdellatief M. Mechanical, microstructural characteristics and sustainability analysis of concrete incorporating date palm ash and eggshell powder as ternary blends cementitious materials. Constr Build Mater. 2024;411:134753.
[19] Jatoi FA, Sahito HA, Shaikh AM. Population density of lesser date moth on most prominent date palm cultivars at Khairpur Mirs. Pak J Biotechnol. 2024;21:305–11.
[20] Valente M, Rossitti I, Sambucci M. Different production processes for thermoplastic composite materials: sustainability versus mechanical properties and processes parameter. Polymers. 2023;15:242.
[21] Xiangji D, Zihao L, Zhigang H. Analysis of the flow field in a meshing and co-rotating differential twin screw extruder for extruding polylactic acid. Food Machinery. 2024;40:59–64.
[22] Szulc A, Skotnicka E, Gupta MK, Królczyk JB. Powder agglomeration processes of bulk materials–A state of the art review on different granulation methods and applications. Powder Technol. 2024;431:119092.
[23] Gale B. Petronas: Malaysia's national oil corporation. Asian Surv. 1981;21:1129–44.
[24] Abass RU, Abass FU, Abas MO. Improvement of mechanical properties of polyester composite reinforced by bio filler (Acro Shell). Int J Innov Sci Eng Technol. 2015;2:35–8.
[25] Kerni L, Singh S, Patnaik A, Kumar N. A review on natural fiber reinforced composites. Mater Today: Proc. 2020;28:1616–21.
[26] Espinach F, Vilaseca F, Tarrés Q, Delgado-Aguilar M, Aguado R, Mutjé P. An alternative method to evaluate the micromechanics tensile strength properties of natural fiber strand reinforced polyolefin composites. The case of hemp strand-reinforced polypropylene. Compos Part B: Eng. 2024;273:111211.
[27] Kassegn E, Sirhabizu B, Berhanu T, Buffel B, Desplentere F. Experimental study on single fiber tensile properties of Sisal fibers using a digital image correlation method as a strain measurement. J Nat Fibers. 2024;21:2325557.
[28] Shen X, Brühwiler E. Influence of local fiber distribution on tensile behavior of strain hardening UHPFRC using NDT and DIC. Cem Concr Res. 2020;132:106042.
[29] Swain PTR, Das SN, Jena SP. Manufacturing and study of thermo-mechanical behaviour of surface modified date palm leaf/glass fiber reinforced hybrid composite. Mater Today: Proc. 2018;5:18332–41.
[30] Al-Oqla FM, Hayajneh MT, Al-Shrida MA. Mechanical performance, thermal stability and morphological analysis of date palm fiber reinforced polypropylene composites toward functional bio-products. Cellulose. 2022;29:3293–309.
[31] Sadek MG, Abdellah MY, Abdel-Jaber GT. A review on properties, applications and feasibility study of date palm fiber-reinforced polymer composites. SVU-Int J Eng Sci Appl. 2024;5:50–61.
[32] Wei J, Abdurexit A, Jamal R, Abdiryim T, You J, Li Z, et al. Carbon fiber reinforced recycled polypropylene/polyolefin elastomer composites with high mechanical properties. Polymers. 2024;16:972.
[33] Mahesh V, Joladarashi S, Kulkarni SM. Damage mechanics and energy absorption capabilities of natural fiber reinforced elastomeric based bio composite for sacrificial structural applications. Def Technol. 2021;17:161–76.
[34] Abas FO, Abass RU. A new micro-composite material of microparticle amalgam/polyvinyl alcohol for teething structures. Iraqi J Sci. 2019;60(11):2321–31. doi: 10.24996/ijs.2019.60.11.2.
[35] Abas FO, Ibrahim SI, Abass RU. Mechanical and thermal properties of heterogonous epoxy-cellulose fiber-micron ceramic particles composite systems. Eng Tech J. 2011;29:1962–70.
[36] Madhurima K, Nandi B, Munshi S, Naganathan AN, Sekhar A. Functional regulation of an intrinsically disordered protein via a conformationally excited state. Sci Adv. 2023;9:eadh4591.
[37] Abid SA, Taha AA, Ismail RA, Mohsin MH. Antibacterial and cytotoxic activities of cerium oxide nanoparticles prepared by laser ablation in liquid. Environ Sci Pollut Res. 2020;27:30479–89. doi: 10.1007/s11356-020-09332-9.
[38] Ismail RA, Khashan KS, Mahdi RO. Characterization of high photosensitivity nanostructured 4H-SiC/p-Si heterostructure prepared by laser ablation of silicon in ethanol. Mater Sci Semicond Process. 2017;68:252–61.
[39] Ismail RA, Al Samarai AME, Muhammed AM. High-performance nanostructured p-Cu2S/n-Si photodetector prepared by chemical bath deposition technique. J Mater Sci: Mater Electron. 2019;30:11807–18. doi: 10.1007/s10854-019-01554-z.
[40] Khashan KS, Ismail RA, Mahdi RO. Synthesis of SiC nanoparticles by SHG 532 nm Nd: YAG laser ablation of silicon in ethanol. Appl Phys A. 2018;124(6):443.
[41] Ismail RA, Mousa AM, Shaker SS. Visible-enhanced silver-doped PbI2 nanostructure/Si heterojunction photodetector: effect of doping concentration on photodetector parameters. Opt Quantum Electron. 2019;51:362. doi: 10.1007/s11082-019-2063-x.
[42] Addie AJ, Ismail RA, Mohammed MA. Amorphous carbon nitride dual-function anti-reflection coating for crystalline silicon solar cells. Sci Rep. 2022;12:9902. doi: 10.1038/s41598-022-14078-0.
[43] Hammadi DF, Adnan A, Al-Sarraf MA. The effect of silicon carbide addition on the transformation temperatures and wear resistance of Cu-based shape memory alloys. Mater Today Proc. Jan. 2022;62:6068–76. doi: 10.1016/j.matpr.2022.04.1010.
[44] Ismail M, Rejab MRM, Siregar JP, Mohamad Z, Quanjin M, Mohammed AA. Mechanical properties of hybrid glass fiber/rice husk reinforced polymer composite. Mater Today: Proc. 2020;27:1749–55. doi: 10.1016/j.matpr.2020.03.660.
[45] Mohammed AA, Bachtiar D, Rejab MRM, Siregar JP. Effect of microwave treatment on tensile properties of sugar palm fibre reinforced thermoplastic polyurethane composites. Def Technol. Aug. 2018;14(4):287–90. doi: 10.1016/j.dt.2018.05.008.
[46] Mohammed AA, Bachtiar D, Rejab MR, Jiang XX, Abas FO, Abass RU, et al. Effects of KMnO4 treatment on the flexural, impact, and thermal properties of sugar palm fiber-reinforced thermoplastic polyurethane composites. JOM. May 2018;70(7):1326–30. doi: 10.1007/s11837-018-2869-1.
[47] Mohammed AA, Bachtiar D, Siregar JP, Rejab MRM. Effect of sodium hydroxide on the tensile properties of sugar palm fibre reinforced thermoplastic polyurethane composites. J Mech Eng Sci. Jun. 2016;10(1):1765–77. doi: 10.15282/jmes.10.1.2016.2.0170.
[48] Abas FO, Abass RU. Study thermo-mechanical properties of polyester composite reinforced by ceramic particles, SiC. MATEC Web Conf. Jan. 2018;225:01021. doi: 10.1051/matecconf/201822501021.
[49] Abasi FO, Aabass RU. Thermo-mechanical behavior of epoxy composite reinforced by carbon and Kevlar fiber. MATEC Web Conf. 2018;225:01022. doi: 10.1051/matecconf/201822501022.
[50] Abas FO, Al Obaidy AH, Awad ES. Preparation of polymer composite membrane reinforced by natural fibers (Fiber and Stem of Date

Palm) for treatment of industrial waste water residue. Theor Found Chem Eng. Sep. 2020;54(5):961–72. doi: 10.1134/s0040579520050267.
[51] Abas FO. Re-use of date palm wastes to improve aging of composite concrete system. Iraqi J Sci. Mar. 2020;225:462–71. doi: 10.24996/ijs.2020.61.3.1.
[52] Barbooti MM, Mohamed TJ, Hussain AA, Abas FO. Optimization of pyrolysis conditions of scrap tires under inert gas atmosphere. J Anal Appl Pyrolysis. Aug. 2004;72(1):165–70. doi: 10.1016/j.jaap.2004.05.001.
[53] Kadri E, Dhahri K, Barillé R, Rasheed M. Novel method for the determination of the optical conductivity and dielectric constant of SiGe thin films using Kato-Adachi dispersion model. Phase Transit. Feb. 2021;94(2):65–76. doi: 10.1080/01411594.2020.1832224.
[54] Alshalal I, Al-Zuhairi HMI, Abtan AA, Rasheed M, Asmail MK. Characterization of wear and fatigue behavior of aluminum piston alloy using alumina nanoparticles. J Mech Behav Mater. Jan. 2023;32(1):2321–31. doi: 10.1515/jmbm-2022-0280.
[55] Bouras D, Fellah M, Barille R, Abdul Samad M, Rasheed M, Awjan Alreshidi M. Properties of MZO/ceramic and MZO/glass thin layers based on the substrate's quality. Opt Quantum Electron. Dec. 2023;56(1):462–71. doi: 10.1007/s11082-023-05778-6.
[56] Bouras D, Rasheed M. Comparison between CrZO and AlZO thin layers and the effect of doping on the lattice properties of zinc oxide. Opt Quantum Electron. Oct. 2022;54(12):1021–8. doi: 10.1007/s11082-022-04161-1.
[57] Ahcen Keziz M, Heraiz F, Sahnoune, Rasheed M. Characterization and mechanisms of the phase's formation evolution in sol-gel derived mullite/cordierite composite. Ceram Int. Oct. 2023;49(20):32989–3003. doi: 10.1016/j.ceramint.2023.07.275.
[58] Al-Darraji M, Jasim S, Salah Aldeen O, Ghasemian A, Rasheed M. The effect of LL37 antimicrobial peptide on FOXE1 and lncRNA PTCSC 2 genes expression in colorectal cancer (CRC) and normal cells. Asian Pac J Cancer Prev. Oct. 2022;23(10):3437–42. doi: 10.31557/apjcp.2022.23.10.3437.
[59] Sellam M, Rasheed M, Azizii S, Saidani T. Improving photocatalytic performance: Creation and assessment of nanostructured SnO2 thin films, pure and with nickel doping, using spray pyrolysis. Ceram Int. Mar. 2024;32(1):1–7. doi: 10.1016/j.ceramint.2024.03.094.
[60] Ahcen Keziz M, Rasheed M, Heraiz F, Sahnoune, Latif A. Structural, morphological, dielectric properties, impedance spectroscopy and electrical modulus of sintered Al6Si2O13–Mg2Al4Si5O18 composite for electronic applications. Ceram Int. Dec. 2023;49(23):37423–34. doi: 10.1016/j.ceramint.2023.09.068.
[61] Jaber AS, Ismael M, Rashid T, Sarhan MA, Rasheed M, Sala IM. Comparesion the electrical parameters of photovoltaic cell using numerical methods. Eureka: Phys Eng. Jul. 2023;27(4):29–39. doi: 10.21303/2461-4262.2023.002770.
[62] Assoudi N, Chaabani A, Rasheed M, Walha I, Dhahri E, Alawsi T, et al. Comparative examination of the physical parameters of the sol gel produced compounds La0.5Ag0.1Ca0.4MnO3 and La0.6Ca0.3Ag0.1MnO3. Opt Quantum Electron. Jul. 2022;54(9):32989–3003. doi: 10.1007/s11082-022-03927-x.
[63] Darraji M, Saqban L, Mutar T, Rasheed M, Hussein A. Association of candidate genes polymorphisms in Iraqi patients with chronic kidney disease. J Adv Biotechnol Exp Ther. 2022;6(1):687. doi: 10.5455/jabet.2022.d147.
[64] Rasheed M, Saleem MM, Marzoog TR, Taki MM, Bouras D, Hashim IA. Effect of caffeine-loaded silver nanoparticles on minerals concentration and antibacterial activity in rats. J Adv Biotechnol Exp Ther. Jan. 2023;6(2):495–509. doi: 10.5455/jabet.2023.d144.
[65] Kherifi D, Keziz A, Rasheed M, Oueslati A. Thermal treatment effects on Algerian natural phosphate bioceramics: A comprehensive analysis. Ceram Int. May 2024;49:37423–34. doi: 10.1016/j.ceramint.2024.05.317.
[66] Hussein AJ, Al-Darraji MN, Rasheed M, Sarhan MA. A study of the characteristics of wastewater on the Euphrates River in Iraq. IOP Conf Ser Earth Environ Sci. Dec. 2023;1262(2):022005. doi: 10.1088/1755-1315/1262/2/022005.
[67] Hussein AJ, Al-Darraji MN, Rasheed M. A study of physicochemical parameters, heavy metals and Algae in the Euphrates River, Iraq. IOP Conf Ser Earth Environ Sci. Dec. 2023;1262(2):022007. doi: 10.1088/1755-1315/1262/2/022007.
[68] Al Zubaidi FN, Asaad LM, Alshalal I, Rasheed M. The impact of zirconia nanoparticles on the mechanical characteristics of 7075 aluminum alloy. J Mech Behav Mater. Jan. 2023;32(1):687–701. doi: 10.1515/jmbm-2022-0302.
[69] Rasheed M, Shihab S, Alabdali O, Rashid A, Rashid T. Finding roots of nonlinear equation for optoelectronic device. J Phys: Conf Ser. Sep. 2021;1999(1):012077. doi: 10.1088/1742-6596/1999/1/012077.
[70] Rasheed M, Alabdali O, Shihab S, Rashid A, Rashid T. On the solution of nonlinear equation for photovoltaic cell using new iterative algorithms. J Phys: Conf Ser. Sep. 2021;1999(1):012078. doi: 10.1088/1742-6596/1999/1/012078.
[71] Rasheed M, Nuhad Al-Darraji M, Shihab S, Rashid A, Rashid T. The numerical calculations of single-diode solar cell modeling parameters. J Phys: Conf Ser. Jul. 2021;1963(1):012058. doi: 10.1088/1742-6596/1963/1/012058.
[72] Alabdali O, Shihab S, Rasheed M, Rashid T. Orthogonal Boubaker-Turki polynomials algorithm for problems arising in engineering. 3rd International Scientific Conference of Alkafeel University (ISCKU 2021). 2022. doi: 10.1063/5.0066860.
[73] Bouras D, Rasheed M, Barille R, Aldaraji MN. Efficiency of adding DD3+ (Li/Mg) composite to plants and their fibers during the process of filtering solutions of toxic organic dyes. Opt Mater. Sep. 2022;131:112725. doi: 10.1016/j.optmat.2022.112725.
[74] Shihab S, Rasheed M, Alabdali O, Abdulrahman AA. A novel predictor-corrector hally technique for determining the parameters for nonlinear solar cell equation. J Phys: Conf Ser. May 2021;1879(2):022120. doi: 10.1088/1742-6596/1879/2/022120.
[75] Rasheed M, Al-Darraji MN, Shihab S, Rashid A, Rashid T. Solar PV modelling and parameter extraction using iterative algorithms. J Phys: Conf Ser. Jul. 2021;1963(1):012059. doi: 10.1088/1742-6596/1963/1/012059.
[76] Rasheed M, Shihab S, Mohammed OY, Al-Adili A. Parameters estimation of photovoltaic model using nonlinear algorithms. J Phys: Conf Ser. Mar. 2021;1795(1):012058. doi: 10.1088/1742-6596/1795/1/012058.
[77] Sarhan MA, Shihab S, Kashem BE, Rasheed M. New exact operational shifted pell matrices and their application in astrophysics. J Phys: Conf Ser. May 2021;1879(2):022122. doi: 10.1088/1742-6596/1879/2/022122.
[78] Bouras D, Fellah M, Mecif A, Barillé R, Obrosov A, Rasheed M. High photocatalytic capacity of porous ceramic-based powder doped with MgO. J Korean Ceram Soc. Oct. 2022;131:112725–34. doi: 10.1007/s43207-022-00254-5.

[79] Rasheed M, Alabdali O, Hassan HH. Parameters extraction of a single-diode model of photovoltaic cell using false position iterative method. J Phys: Conf Ser. May 2021;1879(3):032113. doi: 10.1088/1742-6596/1879/3/032113.
[80] Rasheed M, Mohammed OY, Shihab S, Al-Adili A. Explicit numerical model of solar cells to determine current and voltage. J Phys: Conf Ser. Mar. 2021;1795(1):012043. doi: 10.1088/1742-6596/1795/1/012043.
[81] Enneffatia M, Rasheed M, Louatia B, Guidaraa K, Shihab S, Barillé R. Investigation of structural, morphology, optical properties and electrical transport conduction of Li0.25Na0.75CdVO4 compound. J Phys: Conf Ser. Mar. 2021;1795(1):012050. doi: 10.1088/1742-6596/1795/1/012050.
[82] Saidi W, Hfaidh N, Rasheed M, Girtan M, Megriche A, Maaoui ME. Effect of B2O3addition on optical and structural properties of TiO2 as a new blocking layer for multiple dye sensitive solar cell application (DSSC). RSC Adv. Jan. 2016;6(73):68819–26. doi: 10.1039/c6ra15060h.
[83] Kadri E, Krichen M, Mohammed R, Zouari A, Khirouni K. Electrical transport mechanisms in amorphous silicon/crystalline silicon germanium heterojunction solar cell: impact of passivation layer in conversion efficiency. Opt Quantum Electron. Nov. 2016;48(12). doi: 10.1007/s11082-016-0812-7.